Published by Institute of Physics Publishing for SISSA/ISAS
Received: *January 16, 2003*
Revised: *November 7, 2003*
Accepted: *November 21, 2003*

Measurement of ^{3}He/^{4}He ratio in cosmic rays with the AMS experiment

Zhaohua Xiong

Institute of High Energy Physics, Academia Sinica, Beijing 100039, China, and Graduate School of Science, Hiroshima University 1-3-1 Kagamiyama, Higashi Hiroshima,739-8526, Japan
E-mail: xiongzh@theo.phys.sci.hiroshima-u.ac.jp

Hesheng Chen, Changgen Yang, Min Yang, Guomeng Chen, Gang Chen, Yusheng Lü, Honglin Zhuang and Xiaowei Tang

Institute of High Energy Physics, Academia Sinica
Beijing 100039, China
E-mail: chenhs@sun.ihep.ac.cn, yangcg@mail.ihep.ac.cn, yangm@mail.ihep.ac.cn, chengm@mail.ihep.ac.cn, cheng@mail.ihep.ac.cn, luys@mail.ihep.ac.cn, zhuanghl@mail.ihep.ac.cn, tangxw@mail.ihep.ac.cn

Abstract: The cosmic-ray ^{3}He/^{4}He ratios from 0.09 to 1.2 GeV per nucleon are measured by Alpha Magnetic Spectrometer (AMS) at its precursor mission on board the space shuttle *Discovery* during the flight STS-91 in June 1998. Taking unique advantage of AMS data collected from a large region covering the earth equator, we also studied the magnetic latitude effect on the ratios. Our analysis shows that the relative abundances of ^{3}He and ^{4}He in cosmic rays depend weakly on the magnetic latitude, and given present uncertainties, the observed isotopic composition is generally consistent with the predictions of the standard propagation model of cosmic rays.

Keywords: Gamma and Cosmic Rays.

© SISSA/ISAS 2003

JHEP11(2003)048

Contents

1. Introduction

The information on the interstellar propagation of cosmic rays began with the discovery of the cosmic radiation containing nuclei heavier than helium and the relative abundance of some cosmic ray elements. It is important to note, however, that the nuclei with $Z \geq 3$ constitute only $\sim 1\%$ of cosmic rays. Hence, it is of great importance to determine the propagation history of the much more abundant H and He nuclei. The helium isotope ^{3}He is generally believed to be secondary particles from nuclear interactions of primary cosmic rays with the interstellar medium. The analysis and interpretations of measured ^{3}He/^{4}He ratio by previous balloon-borne experiments such as MASS [1], SMILI [2], IMAX [3], and BESS [4] are generally consistent with the predictions of the standard leaky box model (SLBM) of cosmic-ray transport in the Galaxy [5].[1]

The Alpha Magnetic Spectrometer (AMS) was flown on the space shuttle *Discovery* during flight STS-91 in June, 1998. Precise measurements of electron, positron [9], proton [10] and helium spectra [11] as well as search for the anti-helium [12] in cosmic rays have been published. The AMS group measured both the spectrum above rigidity cutoff ("primary spectrum") and below regidity cutoff ("second spectrum") [11]. In addition, the group presented measurements for the ^{3}He/^{4}He ratios in "second spectrum", and found that in the region near the earth equator, more than ninety percent of helium in the "second spectrum" is ^{3}He. However, the AMS group did not perform the analysis of ^{3}He/^{4}He ratio using measured "primary spectrum" which is the main task of present work.

In this paper we use a total 625,526 event sample taken by AMS to study the ratio ^{3}He/^{4}He from 0.09 to 1.2 GeV per nucleon in cosmic rays. The organization of this paper

[1] There are exceptions given in [6, 7]. However, it is generally accepted that the reanalysis of the same data [8] is superior which is found to be in good agreement with the SLBM prediction.

JHEP11(2003)048

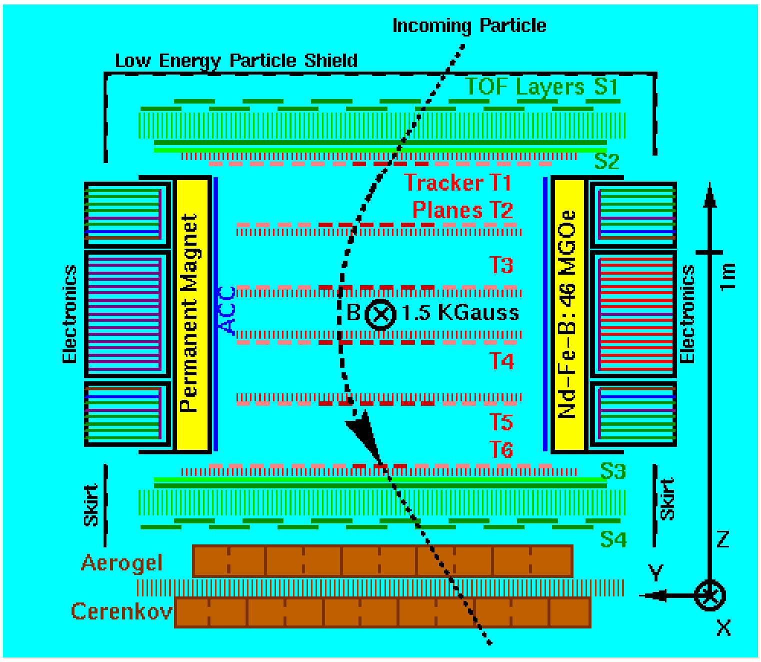

Figure 1: Schematic view of AMS as flown on STS-91 showing the cylindrical permanent magnet, the silicon tracker planes T1 to T6, the time of flight (TOF) hodoscape layers S1 to S4, the aerogel cerenkov counter, the anticoincidence counter(ACC) and low energy particle shields (LEPS).

is follows. Section 2 presents a brief description of AMS detector, where the advantages of AMS data are emphasized. Section 3 describes the detailed event selection and analysis. Section 4 gives the results and interpretation. Section 5 includes our discussions and conclusions.

2. The AMS detector

AMS is a high energy physics experiment scheduled for installation on the Internation Space Station. A schematic cross section in the bending plane of AMS as flown on STS-91 is shown in figure 1 [13].

The permanent magnet has the shape of a cylindrical shell with inner diameter 1.1 m, length 0.8 m. It provides a central dipole field of 0.14 Tesla across the magnet bore and an analyzing power, BL^2, of 0.14 Tm^2 parallel to the magnet or z-axis. The six layers of double sided silicon tracker are arrayed transverse to the magnet axis. The outer layers are just outside the magnet cylinder. The tracker measures the trajectory of relativistic singly charged particles with an accuracy of 20 microns in the bending coordinate and 33 microns in the non-bending coordinate, as well as providing multiple measurements of the energy loss. The time of flight system has two planes at each end of the magnet, covering the outer tracker layers. Together the four planes measure doubly charged particle transit times with an accuracy of 105 psec and also yield multiple energy loss measurements. The Aerogel Cerenkov counter ($n = 1.035$) is used to make independent velocity measurements to separate low energy protons from pions and electrons. A layer of anticoincidence scin-

JHEP11(2003)048

tillation counters lines the inner surface of the magnet to reject the background caused by particles passing through or interacting in the magnet walls and support structures. Low energy particles are absorbed by thin carbon fiber shields.

The detector was simulated using the AMS detector simulation program, based on the GEANT package [14, 15]. The effects of energy loss, multiple scattering, interactions, decays and the measured detector efficiency and resolution were included. After the flight, the AMS detector was also extensively calibrated at two accelerators: at GSI, Darmstadt, with heavy ions (He, C) beams at 600 incident angles and locations and a total of 10^7 events, and at the CERN proton-synchrotron in the energy region of 2 to 14 GeV, with 1200 incident angles and locations and a total of 10^8 events. This ensured that the performance of the detector and the analysis procedure were thoroughly understood.

Compared to balloon-borne experiments, the advantages of data collected by AMS during its precursor mission are the follows:

- High statistics. AMS is the first large magnetic detector in space with large geometric acceptance $\sim 0.3\,\mathrm{m}^2 sr$. A total of 2.86×10^6 helium nuclei observed in the rigidity range 1 to 14 GeV [11, 12] makes the statistic error of the data be neglected safely.

- High altitudes. As an important source of systematic errors, the correction for the effects of atmospheric overburden must be done before comparing the balloon-borne experimental data with the predictions of the model. Differing from this, AMS was flown at altitudes between 320 and 390 km. In this height, the interactions of cosmic helium nuclei with atmosphere are negligible for helium with rigidity above cutoff R_{cutoff} and, therefore, the measured helium spectrum can be compared directly with the model prediction.

- Large region. During AMS data taking, the shuttle varied the latitude range between $\pm 51.7^0$. Data collected in a large region allow to study the geomagnetic latitude effect of cosmic rays.

JHEP11(2003)048

3. Event selection and analysis

The reconstruction of the incident particle type, energy and direction starts with a track finding procedure, which includs cluster finding, cluster coordinate transformation and pattern recognition. The track is then fit using two independent algorithms [16, 17]. For a track to be accepted, the fit is required to include at least 4 hits in the bending plane and at least 3 hits in the non-bending plane. The track is then extrapolated to each TOF plane and matched with the nearest hit if it was within 60 mm, i.e., $S_{\mathrm{TOF}} \leq 60\,\mathrm{mm}$. Matched hits are required in at least three of the four TOF planes. The velocity, $\beta = \mathrm{v}/c$, is then obtained using this TOF information and the trajectory. For events which passed through the Cerenkov counter sensitive volume, an independent velocity measurement, β_C, is also determined. To obtain the magnitude of the particle charge, $|Z|$, a set of reference distributions of energy losses in both TOF and the tracker layers are derived from calibration measurements made at the CERN test beam interpolated via the Monte

Carlo method. For each event, these references are fit to the measured energy losses using a maximum likelihood method. The track parameters are then refit with the measured β and Z. The particle mass is then determined from the resultant Z, β, β_C and rigidity, $R = pc/|Z|e$,

$$m = \frac{RZ}{\beta}(1-\beta^2)^{1/2}\,. \tag{3.1}$$

For this study, a total of 625,526 events recorded in 87 Ntuples with small zenith angle ($\theta_{\mathrm{zenith}} < 1.5^0$) are used.[2] The chosen data have been dealt with preliminarily at CERN. Data taken while orbiting in or near the South Atlantic Anomaly and most $|Z| = 1$ particles have been excluded. In this work, our attentions are focused on the events above cutoff ($R \geq R_{\mathrm{cutoff}}$). To reject fake tracks, in trajectory fitting event with only one track $\mathtt{Npart} = 1$ is accepted. The following selection criteria are also applied to all recorded events to obtain the data used for the helium isotope analysis [18]:

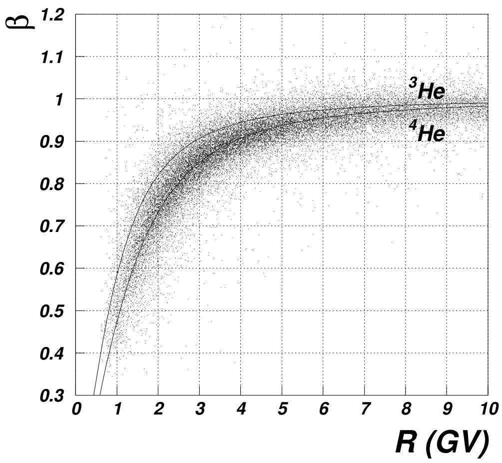

Figure 2: Velocity β as a function of rigidity R. The dots and solid lines stand for the AMS data and the theoretical calculations, respectively.

1. Threefold coincidence for charge of particle determined by pattern recognition, TOF, tracker is required,

$$\mathtt{Pcharge} = \mathtt{ChargeTOF} = \mathtt{ChargeTacker} = 2\,. \tag{3.2}$$

The probability of the wrong charge magnitude assigned by the combined TOF and tracker measurements was estimated to be less than 10^{-7} [12].

2. Velocity β is chosen to be larger than 0.4 and less than 0.9. The theoretical calculation, as shown in figure 2, suggests that in this region ^{3}He and ^{4}He might be distinguishable.

3. Agreement should be satisfied for rigidities obtained from the trajectory fitting by GEANT method, R_G, and fast fit, R, to limit the measured rigidity error. This can be achieved by setting

$$\left|\frac{R_G}{R} - 1\right| \leq 0.5\,. \tag{3.3}$$

The corresponding chisquare of velocity from the trajectory simple fast fit, χ^2_β should be less than 4.

[2]Small zenith angle together with cut 7 (see text) exclude the secondary particles which come from sideway due to incident particle interactions with detector material.

JHEP11(2003)048

4. Agreement for the rigidity obtained from the trajectory fit using first three hits, R_1 and last three hits, R_2, is required to suppress the large angle nuclear scattering events,

$$|A_{12}| \equiv \left| \frac{R_1 - R_2}{R_1 + R_2} \right| \leq 0.45\,. \tag{3.4}$$

5. The number of noise clusters in the silicon tracker is chosen to be less than 8 times effective hits, $N_{\mathrm{trhit}} \leq 8N_{\mathrm{hits}}$, to suppress events with too many noises.

6. Except for the matched hits, no other hits within 5 mm of the track used in trajectory fitting are accepted to reject events with collinear δ electrons from an interaction of the primary particle in the tracker material, that is,

$$S_{\mathrm{Tracker}} > 5\,\mathrm{mm}\,. \tag{3.5}$$

7. No events with total energy deposition in ACC, E_{Anti}, larger than 0.2 MeV are accepted to reject the particle coming from sideway.

We note that for particles coming from above, as shown in figure 1, the amount of material at normal incidence was only $1.5\,\mathrm{g/cm^2}$ in front of the TOF system, and $3.5\,\mathrm{g/cm^2}$ in front of tracker [11]. The most nuclear interactions in this material are rejected by the event selection criteria. The effects of incident ^{4}He particles interacting with this material to produce ^{3}He are thus small and negligible. The efficiency statistics of the criteria are summarized in table 1. They are shown in two columns: the efficiency for each individual cut applied to the data, and the running fraction roughly in the order in which the cuts were applied during the analysis.

To see the roles of the selection criteria clearly, we display the comparisons of the helium mass distribution in figure 3 and the relative mass error distribution in figure 4 before or after selection. It is obvious that the helium mass distribution and mass resolution have been improved greatly.

		Individual cut		Running fraction (%)	
No.	Selection Criterion	Events	Efficiency (%)	Events	Eefficiency (%)
1	Pcharge=chargeTOF= chargeTracker=2	468152	74.84	468152	74.84
2	$0.4 \leq \beta \leq 0.9$	211984	33.89	153159	24.48
3	$\lvert\frac{R_G}{R} - 1\rvert \leq 0.5$, $\chi^2_\beta < 4$	368221	58.87	91317	14.60
4	$\lvert A_{12}\rvert < 0.45$	543481	86.88	90621	14.49
5	$N_{\mathrm{trhit}} \leq 8N_{\mathrm{hits}}$	611064	97.69	89663	14.33
6	$S_{\mathrm{Tracker}} \geq 5\,\mathrm{mm}$	594853	95.10	71437	11.42
7	$E_{\mathrm{Anti}} \leq 0.2\,\mathrm{MeV}$	616552	98.57	71148	11.37

Table 1: Selection Criteria Statistics for the Helium isotope analysis.

JHEP11(2003)048

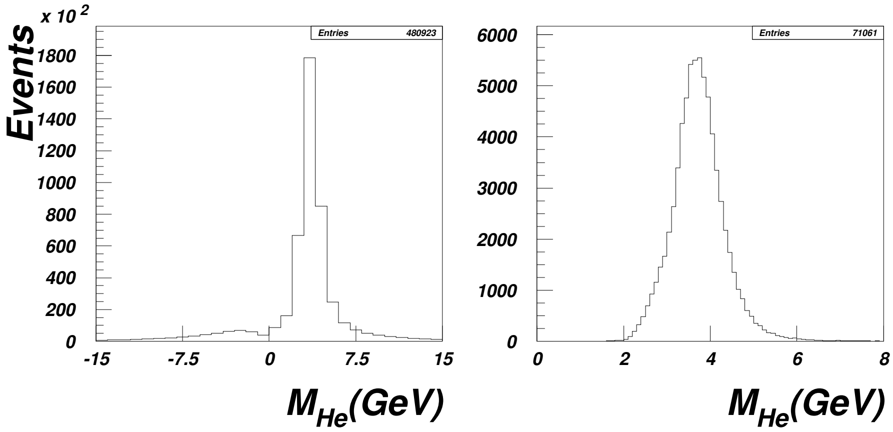

Figure 3: Measured mass distribution before selection (left) and after selection (right) for `pcharge` = 2 particle.

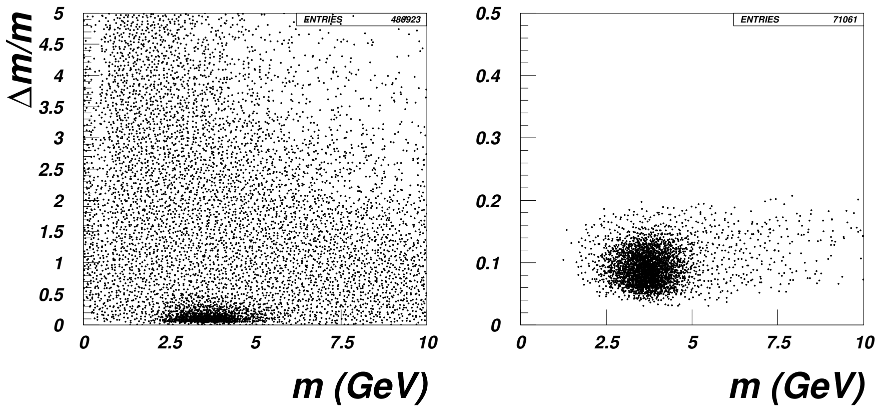

Figure 4: Mass resolution distribution before selection (left) and after selection (right) for `pcharge` = 2 particle.

JHEP11(2003)048

4. Results and interpretation

4.1 Measured ^{3}He/^{4}He ratios

In this study we take gaussian as a good approximation to the mass distribution of helium events,[3] as shown in figure 5. Considering that the helium measured in cosmic rays just consist of ^{3}He and ^{4}He, we extract the corresponding ^{3}He/^{4}He ratios in AMS data from the mean values of the helium mass distributions by fitting. We list the fit mean values and correponding ^{3}He/^{4}He ratios in various kinetic bins in table 2.

[3] The approach is simplistic and prone to systematic errors. Strictly speaking, it should be to model the instrument response to helium events, and fit model helium mass distributions to the observed distributions. Unfortunately, so far no Monte Carlo program on this can be available.

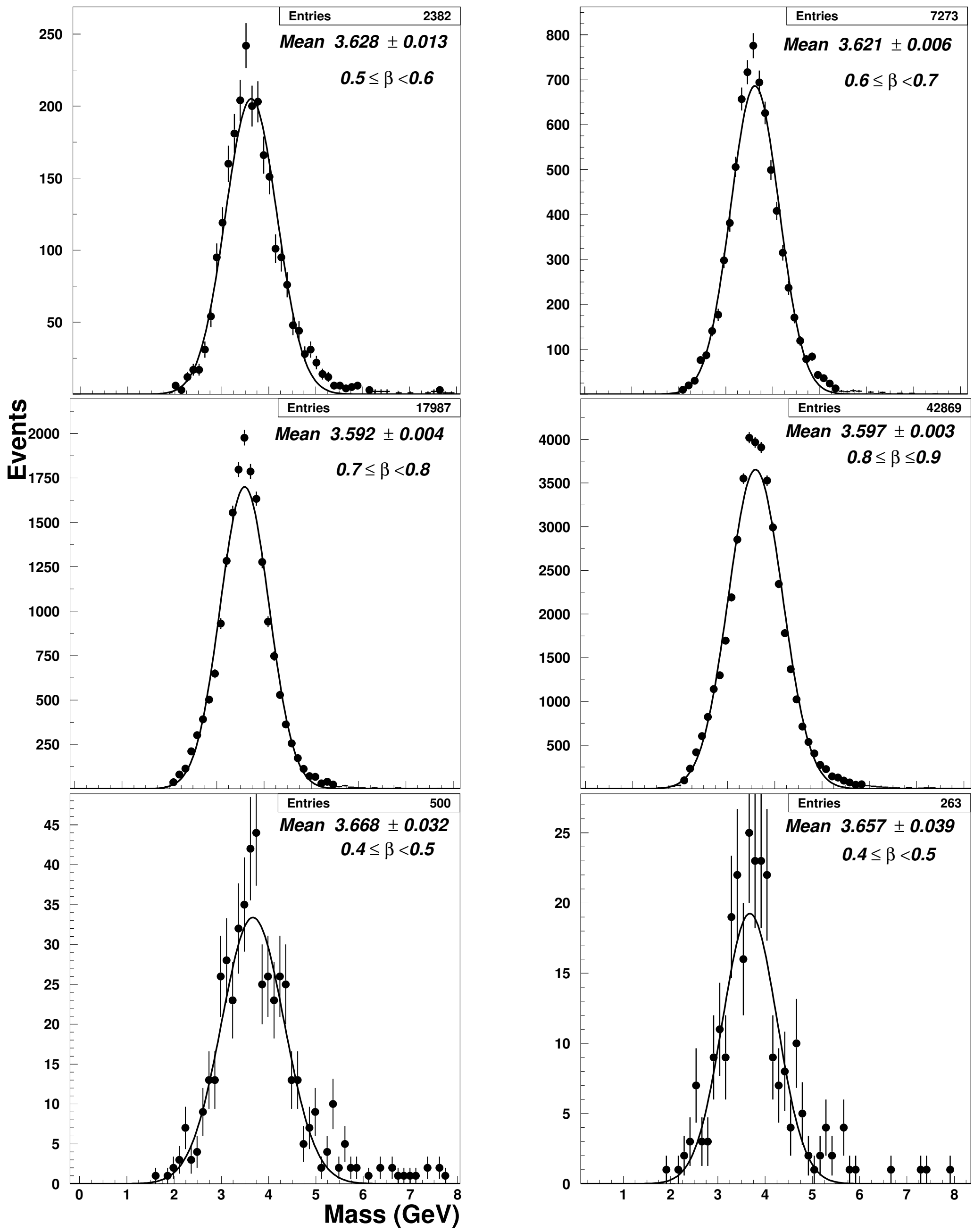

Figure 5: The helium mass distributions in various energy bins. The velocity cutoff β^4_{cutoff} is used for first five diagarms whereas β^3_{cutoff}, in last diagram. The mean values corresponding to given velocity bins obtained by gaussian fit are denoted. The solid lines and dots stand for the gaussian fit and AMS data, respectively.

It is notable that the geomagnetic rigidity cutoff is independent of the charged particle type [19]. Corresponding to R_{cutoff}, the velocity cutoff $\beta_{\text{cutoff}} = ZR_{\text{cutoff}}/\sqrt{m^2+(ZR_{\text{cutoff}})^2}$ depends on the particle mass, which implies that the velocity cutoff for ^{3}He, β^3_{cutoff}, is larger than that for ^{4}He, β^4_{cutoff}, at the same place and incoming angle. Therefore, β^4_{cutoff} should be used in extracting the $^3\text{He}/^4\text{He}$ ratios, as done in fitting the first five diagrams of figure 5.

JHEP11(2003)048

Kinetic energy bin (GeV/nucl)	Events	Fit results: Average masses (GeV)	Fit results: ^{3}He/^{4}He ratios
0.085-0.144	263	3.657 ± 0.039	0.083 ± 0.049(stat.) $\pm$ 0.014(syst.)
0.144-0.233	2382	3.628 ± 0.013	0.121 ± 0.018(stat.) $\pm$ 0.017(syst.)
0.233-0.373	7273	3.621 ± 0.003	0.131 ± 0.004(stat.) $\pm$ 0.010(syst.)
0.373-0.621	17989	3.592 ± 0.004	0.173 ± 0.006(stat.) $\pm$ 0.007(syst.)
0.621-1.205	42869	3.597 ± 0.003	0.165 ± 0.004(stat.) $\pm$ 0.007(syst.)

Table 2: Measured ^{3}He/^{4}He ratios at various energy bins.

Instead, if $\beta^3_{\rm cutoff}$ is used for both ^{3}He and ^{4}He in analysis, it will lead to an underestimated ^{3}He/^{4}He ratio in given kinetic energy (velocity) bin. To see this effect, we assume that the velocity cutoff for ^{4}He is the same as that for ^{3}He, and compare the helium mass distributions with previous ones. We find that the effect of velocity cutoff is negligible compared to the statistical error except for the lowest velocity bin, as indicated in the last diagram of figure 5.

In fact, the selection criteria 2 to 7 in table 1 are little arbitrary, which will induce systematic errors to measured results. In this study, we let the cuts deviate from those listed in table 1 with different degrees according to their distributions and selection efficiencies, say, $\pm 10\%$ deviation for cut 2 and $\pm 20\%$ for other cuts. The same steps are used to get new ^{3}He/^{4}He ratios at various energy bins. For a specified cut, the variation of ^{3}He/^{4}He ratios caused by positive cut deviation may be different from that caused by negative one. In this case, we take larger one as systematic error. Using this approach, we estimate the systematic erros δ_i caused by the deviation from cut i. The total systematic error is then obtained as $\delta = \sqrt{\sum_i \delta_i^2}$. The systematic errors due to the changes of the selection criteria are listed in table 2.

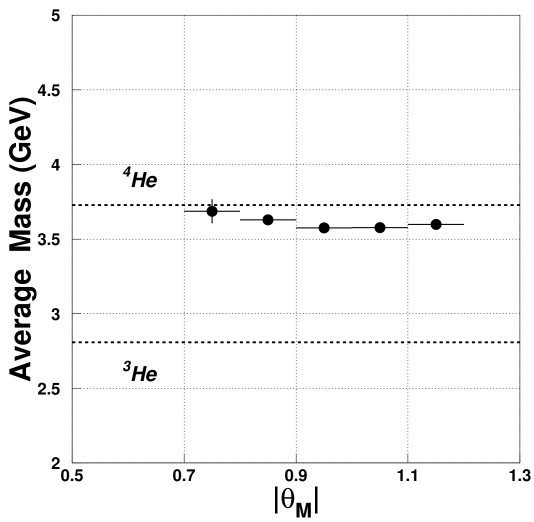

Figure 6: The dependence of average helium mass on the geomagnetic latitude. The dots represent for AMS data.

Now let us turn to the geomagnetic latitude effect. Recalling that AMS has collected data from the latitude range between $\pm 51.7^0$, we take this unique advantage and study the geomagnetic latitude effect on measured ^{3}He/^{4}He ratios. Again we fit the helium mass distribution as a gaussian to obtain the mean value of helium mass in each geomagnetic latitude bin and then extract ^{3}He/^{4}He ratio. The helium mean value as a function of the geomagnetic latitude is displayed in figure 6. From this figure one finds the measured ^{3}He/^{4}He ratio depends weakly on the magnetic latitude θ_M and reach its maximum in the bin $|\theta_M| = 0.9$–1.0.

JHEP11(2003)048

4.2 Interpretation

To test the hypothesis that the origin and the propagation history of Galactic cosmic ray (GCR) helium is identical to that of heavier GCRs, we use the leaky box model of Galactic propagation solved with the weighted slab technique [20]. The weighted slab equations

$$\frac{dN_i}{dx} = \frac{\partial}{\partial E}\left[\left(\frac{dE}{dx}\right)_i N_i\right] - \frac{N_0}{A}\sigma_i N_i + \sum_{j\neq i}\frac{N_0}{A}\sigma_{ij} - \frac{N_i}{\gamma\beta c n \overline{A} T_i} + \sum_{j\neq i}\frac{N_j}{\gamma\beta c n \overline{A} T_j} \tag{4.1}$$

are solved numerically. Here $N_i(E,x)$ is the energy and path length dependent abundance of the ith species; σ_i is the total nuclear spallation cross section; σ_{ij} is the partial nuclear cross section between species i and j; n is the number density of the interstellar material; N_0 is the Avogadro number, and T_i is the half-life of the radioactive species. The local interstellar energy spectrum is obtained by integrating the resultant number density over the path length distribution (PLD),

$$J_i(E) = \int_0^\infty N_i(E,x) PLD(E,x)dx\,. \tag{4.2}$$

In this work we use high precision measurements of B/C ratio [21, 22, 23] to fit an energy-dependent mean PLD, $\lambda_{\rm esc}$. The best fit for $\lambda_{\rm esc}$ is $31.6\beta R^{-0.6}\,{\rm gcm}^{-2}$ for rigidities greater than 4.7 GV, and $12.5\beta\,{\rm gcm}^{-2}$ for lower rigidities, consistent with that used in ref. [3]. The source spectra for all GCRs are taken to be power laws in momentum per nucleon with an index of -2.35 [3, 21] and the source elemental abundances are taken from the *HEAO* 3C-2 analysis [21]. The interstellar medium (ISM) is assumed to be 90% hydrogen and 10% helium by number [24]. The effect of ionized fraction of hydrogen in the ISM [25] is also taken into account.

To describe ^{3}He and ^{4}He cosmic rays interacting with the ISM, the most important inputs for calculation are the mass changing cross sections for ^{3}He and ^{4}He as well as the cross section for the production of ^{3}He from ^{4}He. Using the data from [26, 27] and [28], we parametrized helium mass changing cross sections on hydrogen target as [18]

$$\sigma_{\Delta A\geq 1} = 10\pi r_0^2 (A_B^{1/3} - b)^2 \left[1 - 0.78\exp\left(-\frac{E}{393}\right)\sin(12.8E^{-0.32})\right](mb)\,, \tag{4.3}$$

where the kinetic energy E is in unit of MeV per nucleon, $r_0 = 1.35\,{\rm fm}$, and A_B stands for the mass number of incoming nucleon. The fitted constant b is found to be 0.189 for ^{4}He beam. Since only few measurements are available for ^{3}He beam, we just assume here that the mass changing cross section has the same form as in eq. (4.3). In this case, the value of b is changed to 0.133. These cross sections are scaled by a factor of 2.40 to obtain the cross sections on helium target in the ISM [27, 29].

As cross sections for production of ^{3}He from ^{4}He are involved, due to short half-life (12.26 yr) of ^3H in GCRs decaying into ^{3}He, the ^{3}He and ^3H production cross sections should be combined. Since there are few measurements which exhibit little structure, in this study we regard the cross section for the production of ^{3}He from ^{4}He on hydrogen in the ISM as a constant 54 mb with $\pm$10% error band, as used in ref. [3]. For ^{4}He on ^{4}He

JHEP11(2003)048

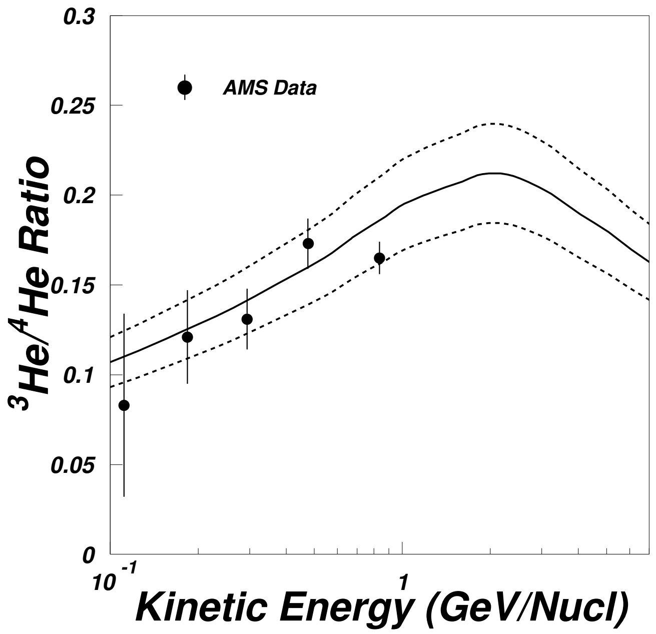

Figure 7: Comparison of measured ^{3}He/^{4}He ratios with the model predictions. The dots correspond to AMS data. The solid line and doted lines denote the propagation model prediction and error bounds, respectively.

reaction, this cross section can be obtained by scaling a target factor of 1.52 [30]. The mass-changing and partial cross sections of ^{3}He and ^{4}He from GCRs with $Z > 2$ are taken from [31] and [32].

To account for the effect of solar modulation on GCR fluxes, we use the spherically symmetric model of the interplanetary medium, including diffusion, convection adiabatic deceleration of GCRs [33]. In this study, we use one parameter ϕ to parameterize solar modulation level. We infer the solar modulation parameter in 1998 to be $\phi \sim 350\,\mathrm{MV}$ by comparing the neutron flux with low energy helium flux (25–93 MeV/nucleon). The former is collected by CLIMAX neutron monitor, while latter by IMP-8 in the period over 1973 to 1993 [34]. For cross check, to extract the factor ϕ during AMS data taking, we take the AMS measured high energy helium spectrum over the rigidity range 20-200 GV [11] as the input unmodulated interstellar spectrum, and compare it to low helium spectrum measured by AMS. The solar modulation factors extracted from two different methods are found to be in good agreement with each other.

A comparison of the model prediction with measured ^{3}He/^{4}He using AMS data is shown is figure 7. The theoretical error bounds derived mainly from uncertainties in λ_{esp}, the mass-changing cross section,$\sigma_{^4\mathrm{He}\to^3\mathrm{He}}$, and the relative target factors, as well as the solar modulation factor ϕ are also plotted. We also compare our results with previous measurements in figure 8. Note that the data in figure 8 correspond to different solar modulation factors. Our measured ^{3}He/^{4}He ratios are generally consistent with previous ^{3}He/^{4}He measurements and the model predictions for given present theoretical and experimental uncertainties.

JHEP11(2003)048

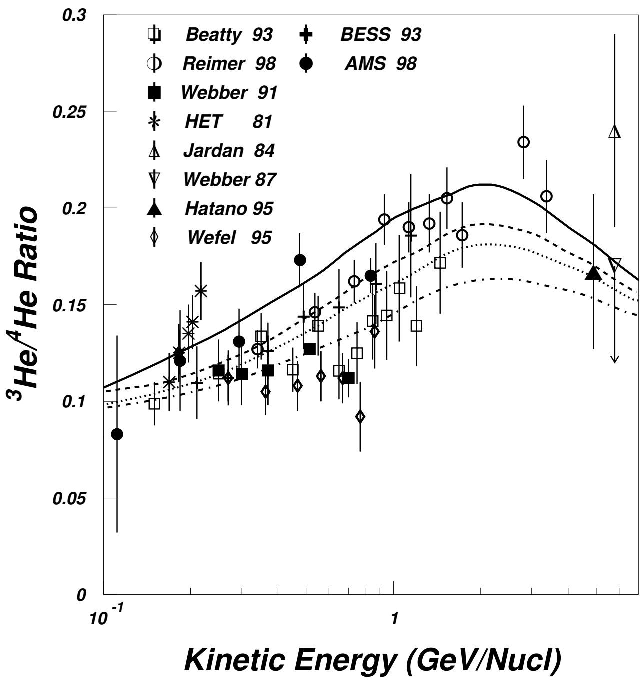

Figure 8: Comparison of measured ^{3}He/^{4}He ratios with previous measurements. The model predictions corresponding to various solar modulation levels are also shown with solid line (ϕ = 0.35 GV), dashed line (ϕ = 0.5 GV), dot line (ϕ = 1 GV), and dot-dashed line (ϕ = 1.5 GV). Data points are as follows: *filled circle*, this work; *filled square*, [1]; *open circle*, [2]; *open square*, [3]; *plus sign*, [4]; *open upward-triangle*, [6], reanalyzed by Webber, Golden and Stephens [8] (*open downward-triangle*); *cross*, [35]; *filled upward-triangle*, [36]; *open diamond*, [37].

5. Conclusions and discussions

The cosmic-ray ^{3}He/^{4}He ratios over the velocity range 0.4–0.9 have been measured using AMS data. The weak dependence of measured ^{3}He/^{4}He ratio on geomagnetic latitude has been found. For given present theoretical and experimental uncertainties, our measurement for the relative abundance of ^{3}He and ^{4}He in cosmic rays is consistent with the standard leaky box model predictions.

After the successful precursor flight (AMS-01), AMS has been improving the detectors: the permanent magnet being replaced by superconducting magnet, the layers of silicon strip tracking detector being increased and the Cerenkov counter being upgraded to the Cerenkov ring image detector. The new detectors, such as electromagnetic calorimeter (ECA) and transit radiation detector (TRD), are also added to AMS. The updated AMS, named AMS-02, will be sent to the international space station. With the improvement of the detectors, more precise data will be available. Therefore, more clear answers to some fundamental physics problems such as antimatter, darkmatter and propagation history of Galactic cosmic rays are expected.

Acknowledgments

We wish to express our gratitude to AMS experiment at CERN, Geneva, Switzerland. We would like to thank Prof. T.P. Li, G.L. Li and J.M. Yang for useful discussions.

JHEP11(2003)048

References

[1] W.R. Webber et al., *A measurement of the cosmic-ray* ^{2}H *and* ^{3}He *spectra and* ^{2}H/^{4}He *and* ^{3}He/^{4}He *ratios in 1989*, *Astrophys. J.* **380** (1991) 230.

[2] J.J. Beatty et al., *The cosmic ray* ^{3}He/^{4}He *ratio from 100 MeV/amu to 1600 MeV/amu*, *Astrophys. J.* **413** (1993) 268.

[3] O. Reimer et al., *The cosmic ray* $^3He/^4He$ *ratio from 200 MeV nucleon to 3.7 GeV nucleon*, *Astrophys. J.* **496** (1998) 490.

[4] J.Z. Wang et al., *Measurement of cosmic-ray Hydrogen and Helium and their isotopic composition with the BESS experiment*, *Astrophys. J.* **564** (2002) 244.

[5] L. Davis, *On the diffusion of cosmic rays in the galaxy*, *Proc. 6th Int. Cosmic-Ray Conf. (Moscow)* **3** (1960) 22;
V.L. Ginzburg and S.I. Syrovatskii, *The origin of cosmic rays* Macmillan, New York 1964;
R. Cowsik, Y. Pal, S.V. Tanddon and R.P. Verma, *Steady state of the cosmic-ray nuclei — their spectral shape and path length at low energies*, *Phys. Rev.* **158** (1996) 1238;
J. Simpson, *Elemental and isotopic composition of the galactic cosmic rays*, *Ann. Rev. Nucl. Sci.* **33** (1983) 328

[6] S.P. Jordan and P. Meyer, *Relative abundance of the helium isotopes* ^{3}He *and* ^{4}He *in the cosmic radiation*, *Phys. Rev. Lett.* **53** (1984) 505.

[7] S.P. Jordan, *The isotopic composition of Helium the cosmic radiation above 11 Gigavolt*, *Astrophys. J.* **291** (1985) 207.

[8] W.R. Webber, R.L. Golden and S.A. Stephens, *Cosmic ray proton and helium spectra from 5-200 GV measured with a magnetic spectrometer*, *Proc. 20th Cosmic Ray Conf. (Moscow)* **1** (1987) 325.

[9] AMS collaboration, J. Alcaraz et al., *Leptons in near earth orbit*, *Phys. Lett.* **B 484** (2000) 10.

[10] AMS collaboration, J. Alcaraz et al., *Protons in near earth orbit*, *Phys. Lett.* **B 472** (2000) 215 [hep-ex/0002049]; *Cosmic protons*, *Phys. Lett.* **B 490** (2000) 27.

[11] AMS collaboration, J. Alcaraz et al., *Helium in near earth orbit*, *Phys. Lett.* **B 494** (2000) 193.

[12] AMS collaboration, J. Alcaraz et al., *Search for antihelium in cosmic rays*, *Phys. Lett.* **B 461** (1999) 387 [hep-ex/0002048].

[13] G.M. Viertel and M. Capell, *The Alpha Magnetic Spectrometer*, *Nucl. Instrum. Meth.* **A419** (1998) 295;
AMS collaboration, J. Alcaraz et al., *The Alpha Magnetic Spectrometer (AMS)*, *Nucl. Instrum. Meth.* **A478** (2002) 119.

[14] R. Brun et al., *GEANT3*, CERN-DD/EE/84-1 1987.

[15] P.A. Aamio et al., *FLUKA users guide*, CERN TIS-RP-190 1990.

[16] J.C. Hart and D.H. Saxon, *Track and vertex fitting in an homogeneous magnetic field*, *Nucl. Instrum. Meth.* **220** (1984) 309.

[17] V. Innocente, M. Marie and E. Nagy, *GEANE: average tracking and error propagation package*, CERN Program Library W5013-E 1991.

JHEP11(2003)048

[18] Z.H. Xiong, *A study of* ^{3}He/^{4}He *ratio in cosmic-rays*, Ph.D. thesis (in chinese), Institute of High Energy Physics, Academia Sinica 2000.

[19] A.E. Sandström, *Cosmic ray physics*, North-Holland Publishing Company, Amsterdam 1965.

[20] M. Garcia-Muñoz et al., *Cosmic-ray propagation in the galaxy and in the heliosphere: the path-length distribution at low energy*, *Astrophys. J. Suppl* **64** (1987) 269.

[21] J.J. Engelmann et al., *Charge composition and energy spectra of cosmic-ray nuclei for elements from* Be *to* Ni *results from HEAO-3-C2*, *Astron. Astrophys.* **233** (1990) 96.

[22] W.R. Webber, A. Lukasiak, F.B. McDonald and P. Ferrando, *New high-statistical-high-resolution measurements of the cosmic-ray CNO isotopes from a 17 year study using the Voyager 1 and 2 spacecraft*, *Astrophys. J.* **457** (1996) 435.

[23] M.E. Wiedenbeck and D.E. Grener, *Isotopic anomalies in the galactic cosmic-ray source*, *Phys. Rev. Lett.* **46** (1981) 682.

[24] R. Protheroe, J.F. Ormes and G.M. Comstock, *Interpretation of cosmic ray composition: the path length distribution*, *Astrophys. J.* **247** (1981) 362

[25] A. Soutoul, P. Ferrando and W.R. Webber, *Proc. 21st int. Cosmic-Ray Conf. (Adelaide)* **3** (1990) 337

[26] J.E. Nicholls et al., *Inelastic p-*^{4}He *scattering at 141 MeV*, *Nucl. Phys.* **A 181** (1972) 329;
R. Klem et al., *Differential cross-sections for p* ^{4}He *elastic scattering at GeV energies*, *Phys. Lett.* **B 70** (1977) 155.

[27] J. Jaros et al., *Nucleus-nucleus total cross-sections for light nuclei at 1.5 GeV/c/nucleon and 2.89 GeV/c/nucleon*, *Phys. Rev.* **C 18** (1978) 2273;
V.G. Abeev et al., *Sov. J. Nucl. Phys.* **36** (1982) 522.

[28] G.N. Vellchko et al., *A superloop approach to supersymmetric gauge theories*, *Nucl. Phys.* **B 193** (1981) 444 [*Sov. J. Nucl. Phys.* **34** (1981) 152] [*Yad. Fiz.* **34** (1982) 270];
Elastic scattering of protons on helium nuclei in the energy range 700-1000 MeV, *Sov. J. Nucl. Phys.* **42** (1985) 837;
W.R. Webber, *New measurements of the cross sections of* ^{4}He *into* ^{2}H *and* 3^{He} *and their implication for* ^{2}H *and* ^{3}He *production in cosmic rays*, *AIP Conf. Proc. 203, Particle Astrophysics*, 1990;
Dubna-Kosice-Moscow-Strasbourg-Tbilisi-Warsaw. collaboration, V.V. Glagolev et al., *Cross-sections of the interactions of* He *nuclei with protons*, *Z. Physik* **C 60** (1993) 421;
S.K. Abdullin et al., *Cross-sections of* ^{4}He *interaction with protons and* ^{4}He *p elastic scattering at 2.7 GeV/C*, *Nucl. Phys.* **A 569** (1994) 753.

[29] D. Lloyd Owen et al., *Total, elastic and inclusive single diffractive cross-sections in* α-α *collisions at the CERN intersecting storage rings*, *Nucl. Phys.* **B 274** (1986) 685.

[30] S.E. Hirzebruch, E. Winkel and W. Heinrich, *Projectile fragmentation cross section for heavy targets*, *Proc. 23th Int. Cosmic Ray Conf. (Galgary)* **2** (1993) 175.

[31] P. Ferrando, et al., *Measurement of* ^{12}C, ^{16}O, *and* ^{56}Fe *charge changing cross-sections in helium at high-energy, comparison with cross-sections in hydrogen, and application to cosmic ray propagation*, *Phys. Rev.* **C 37** (1988) 1490

JHEP11(2003)048

[32] W.R. Webber, J. Kish and D.A. Schrier, *Total charge and mass changing cross-sections of relativistic nuclei in hydrogen, helium, and carbon targets*, *Phys. Rev.* **C 41** (1990) 520; *Individual charge changing fragmentation cross-sections of relativistic nuclei in hydrogen, helium, and carbon targets*, *Phys. Rev.* **C 41** (1990) 533; *Individual isotopic fragmentation cross-sections of relativistic nuclei in hydrogen, helium, and carbon targets*, *Phys. Rev.* **C 41** (1990) 547; *Formula for calculating partial cross-sections for nuclear reactions of nuclei with $e \geq 200\,MeV$/nucleon in hydrogen targets*, *Phys. Rev.* **C 41** (1990) 566

[33] L.A. Fisk, *Solar modulation of galactic cosmic rays*, *J. Geophys. Res.* **76** (1971) 221.

[34] J. Simpson, *Neutrons produced in the atmosphere by the cosmic radiations*, *Phys. Rev.* **83** (1951) 1175;
K. Pyle, *The Haleakala cosmic ray neutron monitor station: Intercalibration with the Huancago station*, *Proc. 23th Int. Cosmic-Ray Conf. (Calgary)* **3** (1993) 609.

[35] W.R. Webber and S.M. Yushak, *A measurement of the energy spectra and relative abundance of the cosmic ray* H *and* He *isotopes over a broad energy range*, *Astrophys. J.* **275** (1983) 391.

[36] Y. Hatano, Y. Fukada, T. Saito, H. Oda and T. Yanagita, *Relative abundance of* ^{3}He *and* ^{4}He *in cosmic rays above 10 GV*, *Phys. Rev.* **D 52** (1995) 6219.

[37] J.P. Wefel, et al., *Measurements of cosmic ray helium during the 1991 solar maximum*, *Proc. 24th Int. Cosmic Ray Conf. (Rome)* **2** (1995) 630

JHEP11(2003)048